



GeO₂/Ge structure submitted to annealing in deuterium: Incorporation pathways and associated oxide modifications

N. M. Bom, G. V. Soares, S. Hartmann, A. Bordin, and C. Radtke

Citation: [Applied Physics Letters](#) **105**, 141605 (2014); doi: 10.1063/1.4898062

View online: <http://dx.doi.org/10.1063/1.4898062>

View Table of Contents: <http://scitation.aip.org/content/aip/journal/apl/105/14?ver=pdfcov>

Published by the [AIP Publishing](#)

Articles you may be interested in

[Kinetic study of GeO disproportionation into a GeO₂/Ge system using x-ray photoelectron spectroscopy](#)
Appl. Phys. Lett. **101**, 061907 (2012); 10.1063/1.4738892

[Postmetallization annealing effect of TiN-gate Ge metal-oxide-semiconductor capacitor with ultrathin SiO₂/GeO₂ bilayer passivation](#)
Appl. Phys. Lett. **98**, 252102 (2011); 10.1063/1.3601480

[Ge nanocrystals embedded in a Ge O_x matrix formed by thermally annealing of Ge oxide films](#)
J. Vac. Sci. Technol. A **27**, 731 (2009); 10.1116/1.3155402

[Effects of fluorine incorporation and forming gas annealing on high-*k* gated germanium metal-oxide-semiconductor with Ge O₂ surface passivation](#)
Appl. Phys. Lett. **93**, 073504 (2008); 10.1063/1.2966367

[Evidence of low interface trap density in Ge O₂/Ge metal-oxide-semiconductor structures fabricated by thermal oxidation](#)
Appl. Phys. Lett. **93**, 032104 (2008); 10.1063/1.2959731

The image shows the cover of an Applied Physics Reviews journal. It features a blue and orange color scheme with a molecular structure background. The text 'NEW Special Topic Sections' is prominently displayed in white. Below it, 'NOW ONLINE' is written in yellow, followed by the title 'Lithium Niobate Properties and Applications: Reviews of Emerging Trends' in white. The AIP Applied Physics Reviews logo is in the bottom right corner.

NEW Special Topic Sections

NOW ONLINE
Lithium Niobate Properties and Applications:
Reviews of Emerging Trends

AIP Applied Physics
Reviews

GeO₂/Ge structure submitted to annealing in deuterium: Incorporation pathways and associated oxide modifications

N. M. Bom,^{1,a)} G. V. Soares,² S. Hartmann,² A. Bordin,² and C. Radtke³

¹PGMICRO, UFRGS, 91509-900 Porto Alegre, Rio Grande do Sul, Brazil

²Instituto de Física, UFRGS, 91509-900 Porto Alegre, Rio Grande do Sul, Brazil

³Instituto de Química, UFRGS, 91509-900 Porto Alegre, Rio Grande do Sul, Brazil

(Received 25 June 2014; accepted 2 October 2014; published online 10 October 2014)

Deuterium (D) incorporation in GeO₂/Ge structures following D₂ annealing was investigated. Higher D concentrations were obtained for GeO₂/Ge samples in comparison to their SiO₂/Si counterparts annealed in the same conditions. Oxygen vacancies produced during the annealing step in D₂ constitute defect sites for D incorporation, analogous to defects at the SiO₂/Si interfacial region. Besides D incorporation, volatilization of the oxide layer is also observed as a consequence of D₂ annealing, especially in the high temperature regime of the present study (>450 °C). In parallel to this volatilization, the stoichiometry and chemical structure of remnant oxide are modified as well. These results evidence the broader impact of forming gas annealing in dielectric/Ge structures with respect to SiO₂/Si counterparts. © 2014 AIP Publishing LLC.
[\[http://dx.doi.org/10.1063/1.4898062\]](http://dx.doi.org/10.1063/1.4898062)

Germanium (Ge) is considered to be an interesting material for replacing Si due to its high charge carrier mobility, narrow bandgap, and low dopant activation temperatures.^{1–5} However, the passivation of the Ge surface is still an issue. Unlike SiO₂ thermally grown on Si, GeO₂ is unstable under temperatures usually employed in device fabrication.¹ As a result, the interfacial quality of GeO₂/Ge structures following usual device processing steps is rather poor, exhibiting high densities of electronic states. Even considering a scenario where the native oxide is replaced by another dielectric with superior physico-chemical properties, Ge substrate oxidation can occur during deposition of the dielectric material and/or device processing.^{6,7} Thus, in order to overcome these problems, an efficient passivation strategy is required.

Si dangling bond (DB), or Pb center, is the key defect at the SiO₂/Si interface. It has been extensively reported that DBs can be passivated by hydrogen (H₂) thermal treatments,^{8–10} where formation of Si-H bonds remove electronic states from the Si bandgap.¹¹ For Ge-based metal-oxide-semiconductor (MOS) structures, it has been shown that H₂ treatments are also efficient to improve electrical characteristics. Forming gas annealing (FGA) of Al₂O₃/Ge^{12,13} and HfO₂/Ge structures^{14,15} was shown to accomplish superior interface quality and to decrease interface state density values. However, the role played by FGA is not clear. Physico-chemical modifications other than DB passivation were proposed as the origin of these electrical improvements: Swaminathan *et al.*,¹³ for example, proposed that oxidation of the Ge substrate induced by the FGA may passivate the interface. Diffusion of Ge into the HfO₂ during FGA may also stabilize higher-k phases of this dielectric layer improving capacitance scaling.¹⁶ Moreover, first-principle calculations predicted the instability of Ge-H bonds at GeO₂/Ge interfaces, implying that DBs are not effectively passivated by FGA.^{17–19} All these results point to a

different effect of FGA on dielectric stacks prepared on Ge in comparison with SiO₂/Si.

Hints of the mechanisms underlying H incorporation in GeO₂ were provided by Ogawa and coworkers,²⁰ who investigated the depth distribution of H within GeO₂ films. They observed high amounts of H incorporated at the GeO₂/Ge interfacial region, as result of thermal treatments under a humid atmosphere. The H concentration decreases as the distance from interface is increased. This behavior was ascribed to the oxygen vacancies sites (Vo), which should be responsible for capturing H mobile related species. The formation of Vo occurs via the GeO₂ + Ge → GeO reaction at the GeO₂/Ge interface. Subsequent diffusion of these vacancies towards the GeO₂ surface promotes desorption of the oxide layer.^{21,22} This process is dominated by O transport, according to an oxygen vacancy diffusion model. In this picture, the concentration of Vo is much higher at the interfacial region. According to this model, it can be concluded that H behavior in GeO₂/Ge structures is related to O transport within these systems.

In this context, we investigated the incorporation of H in GeO₂/Ge upon thermal treatments. As previously described, GeO₂ can be formed, intentionally or not, on the top of the Ge substrate, acting as the major passivation agent. Thus, understanding the effects of H incorporation in this layer is crucial to tailor efficient passivation routes for Ge based devices. The present findings evidence volatilization of GeO₂ induced by H₂ annealing as well as modification of the stoichiometry of this layer.

p-type epitaxial Ge (100) doped with Ga (Umicore) wafers with a resistivity of 0.24–0.47 Ω cm were first cleaned in an ultrasonic acetone bath and then followed a cleaning procedure with H₂O₂ and HCl aqueous solutions.²³ Si (100) samples were cleaned in a mixture of H₂SO₄ and H₂O₂ followed by etching in 40% HF aqueous solution for 1 min. After rinsing the samples in deionized water, they were immediately transferred to load lock chambers. Thermal treatments were performed in a resistively heated quartz tube furnace that was pumped down to 2 × 10⁻⁷ mbar

^{a)} Author to whom correspondence should be addressed. Electronic mail: nicolau.bom@ufrgs.br

prior to pressurization with the gas of interest. All thermal treatments were performed under atmospheric pressure. O_2 enriched to 97% in the ^{18}O rare isotope (termed $^{18}O_2$) was used for thermal oxidations. Samples were submitted to thermal processing under a static atmosphere of deuterium (termed D_2) for 60 min, within the range of 250–550 °C. The use of D_2 and $^{18}O_2$ enabled to employ nuclear reaction techniques to quantify D (natural abundance of 0.015%) and ^{18}O (natural abundance of 0.205%). Besides, we could identify H incorporation exclusively related to the thermal annealing step rather than that originated from ambient contamination. Samples consisting of deposited GeO_2 films were prepared by pulsed DC reactive magnetron sputtering using a Ge target. Argon (Ar) and oxygen (O_2) were introduced in the chamber at a constant flux, keeping the pressure at 4 mTorr during sputtering. Deposition parameters were optimized aiming at a stoichiometric GeO_2 layer as checked by Rutherford backscattering spectrometry (RBS). Each sample prepared on a Ge substrate had a Si counterpart deposited or annealed concurrently. Areal densities of D and ^{18}O were determined by nuclear reaction analysis (NRA) using the plateau regions at 400 keV and 730 keV of $D(^3He,p)^4He$ and $^{18}O(p,\alpha)^{15}N$ nuclear reactions, respectively. Ge amounts on samples prepared on Si substrates were determined by RBS using He^+ ions of 2 MeV. X-ray photoelectron spectroscopy (XPS) was performed with Al K_{α} radiation.

Figure 1(a) shows D areal density as a function of the annealing temperature of thermally oxidized Si and Ge substrates. Following annealing at 250 °C, D was not detected within the sensitivity of the technique. For 350 °C and above, GeO_2/Ge samples incorporate higher amounts of D than their SiO_2/Si counterparts. This observation is probably related to the production of oxygen vacancies in GeO_2/Ge samples which constitute incorporation sites for D. In both cases, a

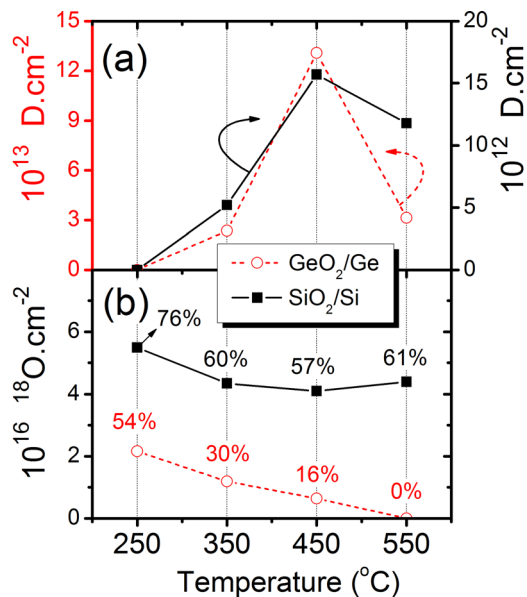


FIG. 1. (a) D areal densities of GeO_2/Ge and SiO_2/Si structures submitted to annealing in D_2 at the indicated temperatures. Both GeO_2 and SiO_2 layers were obtained by thermal oxidation in $^{18}O_2$. (b) Remnant ^{18}O areal densities of the same samples. Above each point is indicated the percentage of ^{18}O concentration of as-oxidized samples, remaining after D_2 annealing. Lines are only to guide the eyes.

maximum of D incorporation is observed for samples annealed at 450 °C. The present results for Si based samples are in agreement with those of Myers²⁴ who stated that the Si-D configuration has a significant activation barrier for formation, being observed only after D_2 exposures above ~ 300 °C. Due to the similar temperature dependence of D uptake of Si and Ge based samples of Fig. 1, one may think that D incorporation and desorption mechanisms are similar in both cases. However, one may remember that in the high temperature range of these curves (450–550 °C), GeO_2 is not stable on Ge. Quantification of the remaining ^{18}O amount of each sample following these treatments was performed to probe the stability of such structures. Fig. 1(b) shows these values as a function of the D_2 annealing temperature. Above each point, the percentage of the ^{18}O concentration of as-oxidized samples (remaining after D_2 annealing) is indicated. Si samples keeps 76% of the original ^{18}O amount following annealing at 250 °C. For higher temperatures, this percentage varies around 60%. The observed ^{18}O losses are probably a result of oxygen isotopic exchange induced by the annealing step.²⁵ A much stronger ^{18}O loss is observed for Ge based samples. Only 54% of the original ^{18}O amount remains following annealing at 250 °C. The higher the annealing temperature, the lower the remnant ^{18}O amount. At 550 °C, ^{18}O is no more detected. Despite possible oxygen isotopic substitution occurring at some point of the sample processing, the lower thermal stability of GeO_2/Ge structures with respect to SiO_2/Si counterparts is clear.

D incorporation in deposited GeO_2 films on both Ge and Si substrates was also investigated. The main objective was to determine the role of the semiconductor substrate, more precisely, how the production of V_O at the GeO_2/Ge interface influences the D uptake. GeO_2 was deposited concomitantly on Si and Ge. The resulting samples were annealed in D_2 in the same temperature range of Fig. 1. D concentrations obtained from these samples are shown in Fig. 2. A similar dependence of D uptake with temperature is observed for both Si and Ge. However, the two set of data seem to be shifted in the horizontal axis, reflecting the role of the semiconductor substrate. Since GeO_2 is more stable on Si than on Ge,²⁶ due to the absence of V_O production at the GeO_2/Si interface, lower GeO_2 volatilization is expected at the high

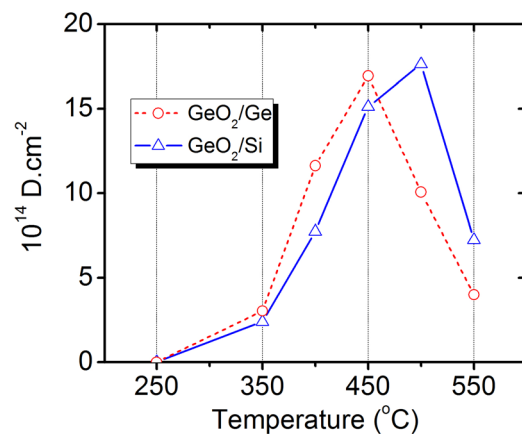
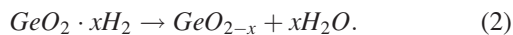
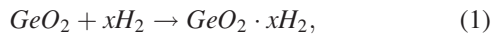


FIG. 2. D areal densities of GeO_2/Si and GeO_2/Ge structures submitted to annealing in D_2 at the indicated temperatures. GeO_2 layers were sputter deposited on Si and Ge substrates. Lines are only to guide the eyes.

temperature range ($>450^\circ\text{C}$). This effect may explain the higher D uptake observed for Si samples. On the other hand, in the lower temperature regime (up to 450°C), where GeO_2 volatilization is not so pronounced, V_O production at the GeO_2/Ge interface may furnish a higher concentration of interaction sites for D_2 . D uptake is the net result of these two processes as shown in Figs. 1 and 2.

It seems that D incorporation and GeO_2 volatilization are directly related to V_O production. This assumption seems to be in contradiction with the results of GeO_2/Si samples where the maximum D uptake is almost identical to the value measured for GeO_2/Ge samples (Fig. 2) (no V_O is formed at the GeO_2/Si interface as evidenced by isotopic tracing studies²⁶). Besides, GeO_2 volatilization should be suppressed when GeO_2 is deposited on Si substrates. However, Fig. 3(a) shows that GeO_2 volatilization was indeed observed in GeO_2/Si samples. Pronounced Ge loss is observed at 450°C , reaching approximately 50% of the original Ge concentration following annealing at 550°C . These results evidence that GeO_2/Si and GeO_2/Ge structures behave similarly with respect to oxide stability and that an agent other than V_O s formed at the GeO_2/Ge interface is responsible for the observed thermal instability. Due to its reduction properties, the D_2 atmosphere can play this role. H_2 interaction with GeO_2 was previously investigated.²⁷ The following reaction scheme was proposed:



The reactions evidence that exposure of GeO_2 to H_2 leads first to the formation of a $\text{GeO}_2 \cdot x\text{H}_2\text{O}$ complex, then to the splitting of the oxygen and the creation of nonstoichiometric oxide. In this way, H_2 exposure would extract O from GeO_2 ,

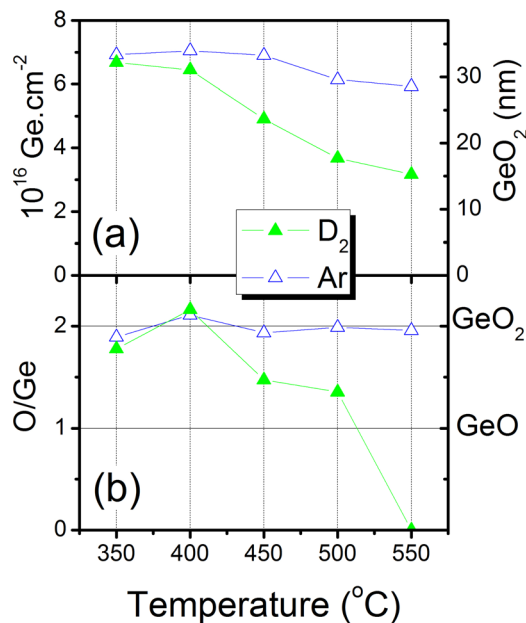


FIG. 3. (a) Ge areal densities of GeO_2/Si structures submitted to annealing in D_2 or Ar at the indicated temperatures. GeO_2 layers were sputter deposited on Si substrates. The right vertical axis corresponds to the respective oxide thickness obtained assuming a GeO_2 density of 3.6 g/cm^3 . (b) O/Ge atomic ratios of the same samples. Lines are only to guide the eyes.

resulting in H incorporation and additional volatilization of the oxide film. The latter could be a result of the production of V_O s followed by disproportionation of the substoichiometric oxide.²⁸ In order to validate the role played by the D_2 atmosphere, we prepared another set of GeO_2/Si samples replacing D_2 by an inert gas, namely Ar. The remnant Ge concentrations on these samples as determined by RBS are shown in Fig. 3. Following the harshest annealing condition at 550°C , approximately 85% of the original Ge amount stays on the substrate in clear contrast to the sample annealed in D_2 at the same conditions. This is a clear evidence of the reducing role of D_2 , which destabilizes GeO_2 and promotes its volatilization.

Besides volatilization of the oxide layer, D_2 annealing may also change the composition and chemical structure of the remnant film. Fig. 3(b) shows the O/Ge ratios of the same samples. O and Ge concentrations were determined by RBS measurements. GeO_2/Si samples annealed in Ar present ratios around 2, indicating that, even following the harshest annealing, the stoichiometry still corresponds to that of GeO_2 . In contrast, D_2 annealing induces reduction of the GeO_2 layer: substoichiometric Ge oxide is already obtained following annealing at 450°C . At 550°C , O is no more detected within the sensitivity of the technique. Fig. 4 shows Ge 3d regions of XPS spectra of samples following D_2 annealing. Samples annealed up to 400°C present two components related to GeO_2 and to substoichiometric species. Above 400°C , the relative intensity of the GeO_x component with respect to the GeO_2 raises, in agreement with the O depletion observed by RBS. At 500°C , an intense component with binding energy

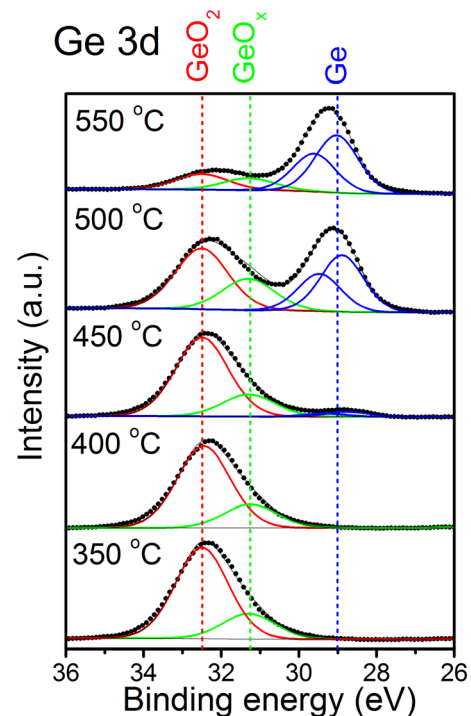


FIG. 4. Ge 3d regions of XPS spectra corresponding to GeO_2/Si structures submitted to annealing in D_2 at the indicated temperatures. GeO_2 layers were sputter deposited on Si substrates. Solid curves correspond to fitting components and their sum. A Shirley background was subtracted from all spectra. The energy position of components assigned to GeO_2 , GeO_x , and Ge are indicated. a.u. stands for arbitrary units.

characteristic of metallic Ge is observed. Its relative intensity rises with the annealing temperature. These results evidence the progressive reduction of the remnant germanium oxide film following annealing in D₂.

A clear modification of the GeO₂ layer following annealing in D₂ was observed for both Si and Ge based samples. However, the GeO₂ growth method (thermal growth or sputtering) could play a role in this process. GeO₂ sputter deposited is more defective than thermally grown GeO₂. This fact explains the higher D amounts observed for GeO₂ layers prepared by thermal oxidation (Fig. 1) with those sputter deposited (Fig. 2), even considering the higher thickness of deposited oxides (at least 3 times thicker than those thermally grown). Thus, the decrease of O amounts within GeO₂ due to D₂ annealings could be ascribed to the more defective nature of the deposited samples rather than the reduction reactions proposed in Eqs. (1) and (2). In order to confirm the role played by D₂, GeO₂/Si samples were once again submitted to D₂ annealings at 550 °C. Nevertheless, aiming at improving the quality of the GeO₂ layers, they were pre-annealed for 60 min under the following conditions: (i) 1 atm of O₂ at 350 °C and (ii) 1 atm of Ar at 550 °C. The remnant O and Ge concentrations obtained by RBS reveal that, even after a pre-annealing step, the stoichiometry of the oxide layer is changed: the O/Ge ratios decreased to 0.66 (O₂ pre-treatment) and to 0.30 (Ar pre-treatment).

The results of D uptake obtained here for GeO₂/Ge are in contrast to those obtained for SiO₂/Si structures. In the latter case, D passivates interface defects and incorporates in the near-interface oxide.²⁹ Deuterium (hydrogen) incorporation in these structures is due to interactions of molecular D₂ with pre-existing defect sites rather than chemical reactions involving the breaking of Si-O bonds. Myers²⁴ compared the D uptake in SiO₂ layers submitted or not to irradiation with high-energy He ions. The irradiation step increased the D uptake by two orders of magnitude, confirming the role of defects in D incorporation. In the case of GeO₂/Ge, a much higher D uptake is observed with respect to SiO₂/Si samples prepared in the same annealing conditions. Comparing Ge-H and Ge-O bond enthalpies (Ge-H ≤ 321.8 kJ/mol and Ge-O 658.1 kJ/mol, Ref. 30) with those of Si-H and Si-O (Si-H ≤ 299.2 kJ/mol and Si-O 809.6 kJ/mol, Ref. 30), it is reasonable to state that D incorporation should be similar in both cases: no breaking of oxide bonds during D₂ annealing and D incorporation in defective sites. One should keep in mind that these values may differ considerably from the real bond energies in the solid state. However, they suggest that a higher concentration of defects in the oxide layer results in a higher D incorporation. Following this reasoning, V_O production at both the GeO₂ surface (induced by D₂ annealing) and at the GeO₂/Ge interface may create interaction sites for D₂.

In summary, D incorporation in GeO₂/Ge structures following D₂ annealings was investigated. Higher D concentrations were obtained for GeO₂/Ge samples in comparison to their SiO₂/Si counterparts annealed in the same conditions. V_Os produced during the annealing step in D₂ constitute defect sites for D incorporation analogous to defects at the SiO₂/Si interfacial region. These vacancies are created both at the GeO₂/Ge interface and at the GeO₂ surface. The latter mechanism results from the interaction of D₂ with the oxide.

Besides D incorporation, volatilization of the oxide layer is also observed following D₂ annealing, especially in the high temperature regime of the present study (>450 °C). In parallel to this volatilization, oxide stoichiometry is also modified: reduction of GeO₂ to metallic Ge takes place. All these results constitute important benchmarks to the choice of FGA parameters of Ge based devices. They also provide a deeper insight into the physico-chemical modifications and related electrical characteristics of Ge MOS structures submitted to FGA.

This work was funded by INCT Namitec, INCT INES, MCT/CNPq, CAPES, and FAPERGS.

- ¹Y. Kamata, *Mater. Today* **11**, 30 (2008).
- ²Y. L. Chao, S. Prussin, J. C. S. Woo, and R. Scholtz, *Appl. Phys. Lett.* **87**, 142102 (2005).
- ³A. Lubow, S. Ismail-Beigi, and T. P. Ma, *Appl. Phys. Lett.* **96**, 122105 (2010).
- ⁴R. Pillarisetty, *Nature* **479**, 324 (2011).
- ⁵E. Simoen, J. Mitard, G. Hellings, G. Eneman, B. De Jaeger, L. Witters, B. Vincent, R. Loo, A. Delabie, S. Sioncke, M. Caymax, and C. Claeys, *Mater. Sci. Semicond. Process.* **15**, 588 (2012).
- ⁶C. Radtke, C. Krug, G. V. Soares, I. J. R. Baumvol, J. M. J. Lopes, E. Durgun-Ozben, A. Nichau, J. Schubert, and S. Mantl, *Electrochem. Solid-State Lett.* **13**, G37 (2010).
- ⁷N. M. Bom, G. V. Soares, C. Krug, I. J. R. Baumvol, and C. Radtke, *Nucl. Instrum. Methods Phys. Res. B* **273**, 146 (2012).
- ⁸K. L. Brower and S. M. Myers, *Appl. Phys. Lett.* **57**, 162 (1990).
- ⁹A. Stesmans, *J. Appl. Phys.* **88**, 489 (2000).
- ¹⁰K. L. Brower, *Phys. Rev. B* **38**, 9657 (1988).
- ¹¹A. H. Edwards, *Phys. Rev. B* **44**, 1832 (1991).
- ¹²C.-C. Cheng, C.-H. Chien, G.-L. Luo, J.-C. Liu, C.-C. Kei, D.-R. Liu, C.-N. Hsiao, C.-H. Yang, and C.-Y. Chang, *J. Electrochem. Soc.* **155**, G203 (2008).
- ¹³S. Swaminathan, M. Shandalov, Y. Oshima, and P. C. McIntyre, *Appl. Phys. Lett.* **96**, 082904 (2010).
- ¹⁴V. V. Afanas'ev, Y. G. Fedorenko, and A. Stesmans, *Appl. Phys. Lett.* **87**, 032107 (2005).
- ¹⁵R. Xie, W. He, M. Yu, and C. Zhu, *Appl. Phys. Lett.* **93**, 073504 (2008).
- ¹⁶Y. Oshima, M. Shandalov, Y. Sun, P. Pianetta, and P. C. McIntyre, *Appl. Phys. Lett.* **94**, 183102 (2009).
- ¹⁷J. R. Weber, A. Janotti, P. Rinke, and C. G. Van de Walle, *Appl. Phys. Lett.* **91**, 142101 (2007).
- ¹⁸M. Houssa, G. Pourtois, V. V. Afanas'ev, and A. Stesmans, *Appl. Phys. Lett.* **99**, 212103 (2011).
- ¹⁹K. Xiong, L. Lin, J. Robertson, and K. Cho, *Appl. Phys. Lett.* **99**, 032902 (2011).
- ²⁰S. Ogawa, T. Suda, T. Yamamoto, K. Kutsuki, and I. Hideshima, *Appl. Phys. Lett.* **99**, 142101 (2011).
- ²¹S. K. Wang, K. Kita, C. H. Lee, T. Tabata, T. Nishimura, K. Nagashio, and A. Toriumi, *J. Appl. Phys.* **108**, 054104 (2010).
- ²²S. K. Wang, K. Kita, T. Nishimura, K. Nagashio, and A. Toriumi, *Jpn. J. Appl. Phys., Part 1* **50**, 04DA01 (2011).
- ²³H. Okumura, T. Akane, and S. Matsumoto, *Appl. Surf. Sci.* **125**, 125 (1998).
- ²⁴S. M. Myers, *J. Appl. Phys.* **61**, 5428 (1987).
- ²⁵I. J. R. Baumvol, *Surf. Sci. Rep.* **36**, 1 (1999).
- ²⁶S. R. M. da Silva, G. K. Rolim, G. V. Soares, I. J. R. Baumvol, C. Krug, L. Miotti, F. L. Freire, Jr., M. E. H. M. da Costa, and C. Radtke, *Appl. Phys. Lett.* **100**, 191907 (2012).
- ²⁷J. J. Zuckerman and A. P. Hagen, "Inorganic reactions and methods," in *Formation of Bonds to C, Si, Ge, Sn, Pb* (VCH Publishers, New York, 1991), Vol. 9, pp. 34–36.
- ²⁸S. K. Wang, H.-G. Liu, and A. Toriumi, *Appl. Phys. Lett.* **101**, 61907 (2012).
- ²⁹I. J. R. Baumvol, E. P. Gusev, F. C. Stedile, F. L. Freire, Jr., M. L. Green, and D. Brasen, *Appl. Phys. Lett.* **72**, 450 (1998).
- ³⁰R. C. Weast, *CRC Handbook of Chemistry and Physics* (CRC Press, Boca Raton, 1985), pp. F174–F179.